SCIENTIFIC REPORTS

OPEN

SUBJECT AREAS:
DIODE LASERS
NONLINEAR PHENOMENA

Received
28 January 2014

Accepted
31 March 2014

Published
15 April 2014

Correspondence and requests for materials should be addressed to A.A. (andres.aragoneses@upc.edu)

Unveiling the complex organization of recurrent patterns in spiking dynamical systems

Andrés Aragoneses[1], Sandro Perrone[1], Taciano Sorrentino[1,2], M. C. Torrent[1] & Cristina Masoller[1]

[1]Departament de Física i Enginyeria Nuclear, Universitat Politécnica de Catalunya, Colom 11, Terrassa, 08222 Barcelona, Spain, [2]Departamento de Ciências Exatas e Naturais, Universidade Federal Rural do Semi-Árido, 59625-900 Mossoró, RN, Brazil.

Complex systems displaying recurrent spike patterns are ubiquitous in nature. Understanding the organization of these patterns is a challenging task. Here we study experimentally the spiking output of a semiconductor laser with feedback. By using symbolic analysis we unveil a nontrivial organization of patterns, revealing serial spike correlations. The probabilities of the patterns display a well-defined, hierarchical and clustered structure that can be understood in terms of a delayed model. Most importantly, we identify a minimal model, a modified circle map, which displays the same symbolic organization. The validity of this minimal model is confirmed by analyzing the output of the forced laser. Since the circle map describes many dynamical systems, including neurons and cardiac cells, our results suggest that similar correlations and hierarchies of patterns can be found in other systems. Our findings also pave the way for optical neurons that could provide a controllable set up to mimic neuronal activity.

Nature presents many fascinating complex systems in which distinguishing signatures of determinism in their high-dimensional dynamics is extremely challenging[1–4], not only because of the presence of noise, but also, because of lack of information about the system: one can measure only one or few relevant variables, and with a limited spatial and/or temporal resolution. A successful approach for studying such systems is by focusing on an event-level description of their dynamics, considering, for example, intervals between events. Examples of this approach include neuronal inter-spike intervals, heart beat-to-beat intervals, earthquake waiting times, intervals between peak communication activity in social networks, etc.[5–10]. For the analysis of these events the symbolic method known as ordinal analysis[11–14] considers the relative order in which the events occur.

Here we use ordinal analysis to study the spiking output of a stochastic optical system, consisting of a semiconductor laser with feedback from an external reflector. Close to the lasing threshold, moderate feedback levels induce apparently random spikes in the laser output intensity, which become more frequent as the laser pump current is increased (see Figs. 1a and 1b). In spite of the fact that the spiking dynamics (referred to as low-frequency-fluctuations, LFFs) has attracted a lot of attention in the last decades[15], several features of the dynamics remain poorly understood, in particular, the presence of correlations in the spike sequence, and how these correlations change as a control parameter, such as the laser pump current, is varied. The well-known Lang and Kobayashi (LK) model[16] predicts that, for typical parameters, the LFF is a transient dynamics sustained by spontaneous emission noise, and the duration of the deterministic transient increases with the pump current[17,18]. Therefore, the presence of correlations in the spike sequence is the fingerprint of the underlying attractor. The main goals of our work are to characterize the symbolic dynamics underlying the spike sequence in order to infer spike correlations, to test whether simulations of the stochastic LK model also display similar correlations, and to investigate if a similar behavior can be observed in other natural systems; specifically, we aim to answer the question whether in sequences of optical spikes there are serial correlations similar to those present in spike sequences of biological neurons.

With these aims we analyze experimentally recorded sequences of optical spikes and unveil a hierarchical and clustered organization of ordinal patterns (in the following referred to as *words*), with a well defined structure of the probabilities of occurrence. Simulations of the LK model are found to be in good agreement with the observations. To the best of our knowledge, ours is the first demonstration of an organized symbolic structure underlying the LFF dynamics, revealing serial correlations among several consecutive intensity dropouts.

Most importantly, we identify a minimal iterative model, a modified circle map (proposed in[19] to represent spike correlations in sensory neurons) that, despite its simplicity, displays a symbolic dynamics with the same

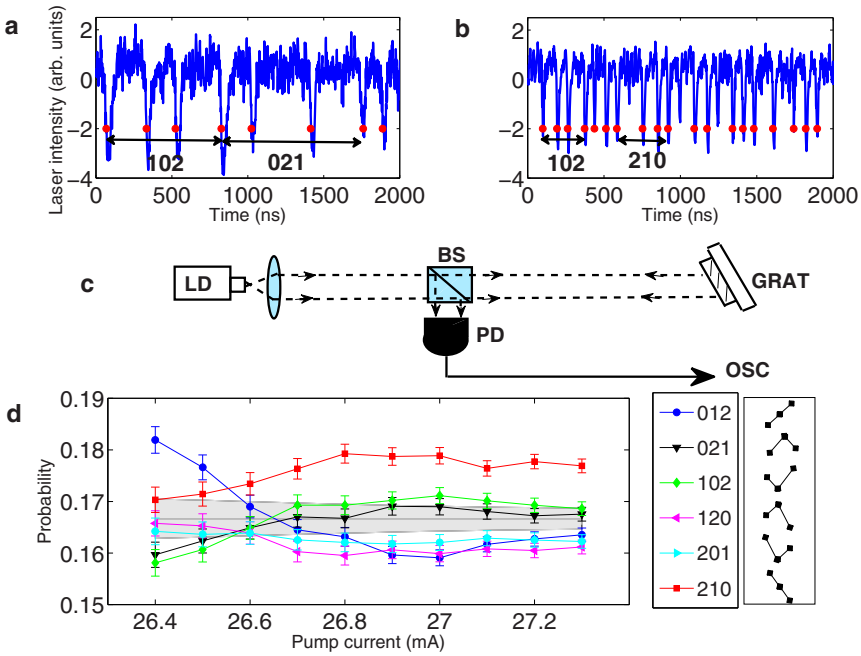

Figure 1 | Spiking laser output, experimental setup, and word probabilities. (a, b), Experimental time trace of the laser intensity when the pump current is 26.5 mA and 27.3 mA respectively. The red dots indicate the spike times and a few ordinal patterns (words) are indicated as examples. (c), Experimental setup, where LD stands for laser diode, BS for beamsplitter, PD for photodetector, OSC for oscilloscope and GRAT for grating (see Methods). (d), Probabilities of the six words (schematically indicated in the right panel) vs the laser pump current. Two clusters of words can be observed, with similar probabilities: 021-102 (black-green) and 120-201 (magenta-cyan). A crossover in the hierarchical organization of the words occurs at about 26.6 mA: at lower current values the word 012 (blue) is the most probable one, while at higher currents values, the word 210 (red) is the most probable one. The error bars are estimated with a binomial test and the gray region indicates probability values consistent with the null hypothesis that there are no correlations in the spike sequence, and therefore, the six words are equally probable[19].

hierarchical and clustered organization of patterns as the experimental data. In order to confirm that this minimal model indeed represents the symbolic dynamics underlying the sequence of optical spikes, we consider the spiking output of the laser with periodic forcing (via a direct modulation of the pump current). We demonstrate that the symbolic dynamics of the forced laser is also in good qualitative agreement with the symbolic dynamics of the modified circle map.

Results

The experimental setup (schematically shown in Fig. 1c and described in Methods) uses a commercial, inexpensive semiconductor laser. We recorded long sequences of optical spikes and analyzed the inter-spike intervals, $\{\Delta T_i = t_{i+1} - t_i\}$, with t_i being the time when a spike occurs. The data contains 70,000–300,000 spikes, at low and high pump current respectively. In the Supplementary Information the threshold criterium used to define the spike times is discussed, and the underlying symbolic organization is shown to be robust to threshold variations.

We construct the ordinal patterns (words) with $D = 3$ consecutive intervals (four consecutive optical spikes) as described in Methods. In Figs. 1a and 1b a few words are indicated as examples. Results for $D = 2$ (and $D = 4$) are presented in the Supplementary Information. Figure 1d displays the probabilities of the six possible words (indicated in the right panel of Fig. 1d), computed from time-series recorded within a wide range of pump currents. The symbolic analysis reveals that serial correlations among four consecutive spikes are present in the spike sequence: if there are no correlations (null hypothesis, represented as gray region in Fig. 1d), the six words are equally probable; however, in Fig. 1d one can observe that the probabilities are clearly not consistent with the null hypothesis.

Moreover, one can observe a hierarchy in the probability values, which presents a crossover at about 26.6 mA: for higher pump currents the most probable word is 210 (corresponding to three consecutively decreasing inter-spike intervals), while for lower pump currents, the most probable word is 012 (corresponding to three consecutively increasing intervals).

Figure 1d also reveals a clustered organization of the probabilities: words 021 and 102, on the one hand, and words 120 and 201, on the other hand, occur with similar probability. The probabilities of these two pairs of words present the same evolution when the pump current is varied. The robustness of these findings was confirmed by using different lasers and feedback conditions (see Supplementary Information), where the same clustered hierarchical structure was found; in fact it can also be observed in Fig. 2b of[20].

To further check the robustness of our observations, we performed simulations of the LK model[16] (see Methods). The model predicts a fast pulsing behavior, in the picosecond time-scale that, after being properly filtered out (to account for the bandwidth of experimental measurements), gives a sequence of spikes in good agreement with the observations.

Figures 2a and 2b show the numerically calculated word probabilities vs the laser pump current parameter of the model, μ, for two sets of parameters. The simulations agree qualitatively well with the experimental findings: we observe the same hierarchical and clustered organization of patterns, as well as the same crossover. Figures 2a and 2b also point to the robustness of the results, as the two clusters are present in simulations with different feedback strengths.

A relevant question is whether the hierarchical and clustered organization of symbolic patterns uncovered here also occurs in other natural systems. If this is the case, there should be a minimal model that also displays such organization of ordinal patterns. We analyzed the symbolic dynamics of several iterative maps and found one, surprisingly simple, a modified circle map (see Methods), that reproduces the hierarchy and clustered organization of the word

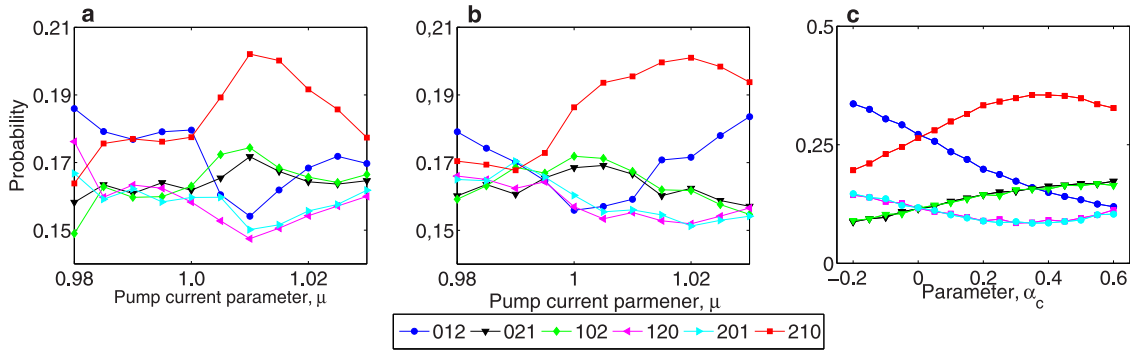

Figure 2 | Probabilities of the ordinal patterns calculated numerically. (a, b), The probabilities are computed from simulations of the LK model; the feedback strength is $\eta = 10$ ns^{-1} and 20 ns^{-1} respectively; other model parameters are as indicated in Methods. (c), Probabilities computed from the minimal model, Eq. (3). The parameters are: $\rho = 0.23$, $K = 0.04$ and $\beta_c = 0.002$. Both, in the LK model and in the minimal model, the hierarchy in the word probabilities, the clustering and the crossover are the same as in the experimental data, Fig. 1d.

probabilities. Figure 2c shows the probabilities obtained from the modified circle map vs the map parameter, α_c. We note that the effect of varying α_c corresponds, qualitatively, to varying the laser pump current: a similar behavior as in Figs. 1d, 2a and 2b can be observed. There is the same hierarchy in the probabilities, which undergoes the same crossover. The existence of the two clusters is also remarkable, formed by the same words as in the sequence of optical spikes.

To further demonstrate that the modified circle map is a minimal model for the spiking laser output, we consider the laser response to a periodic forcing. Figures 3a, 3b display typical time traces of the laser output with direct pump current modulation, and Fig. 3c displays the experimental setup (see Methods). In Fig. 3a, the effect of weak forcing can be clearly observed and, as the forcing increases, the spikes synchronize with the forcing and the inter-spike intervals become multiples of the modulation period, Fig. 3b[21,22].

Figure 4a displays the word probabilities computed from the experimental data, as a function of the modulation amplitude. We observe that, despite the external forcing acting on the system, the symbolic dynamics has the same two clusters as in the unperturbed case (021-102 and 120-201). Also a clear hierarchy is manifested in the probabilities, which present a crossover too, at about 2% of modulation amplitude. For strong modulation the hierarchy of patterns is modified, with words 012 and 210 now being the less probable ones. This can be understood by considering that the modulation imposes a "rhythm" in the spike sequence and consecutively decreasing or increasing inter-spike intervals are less probable as they imply that the synchrony with the external rhythm is lost, either because the spikes are increasingly close ($\Delta T_i > \Delta T_{i+1} > \Delta T_{i+2}$ representing word 210), or because the spikes are increasingly separated ($\Delta T_i < \Delta T_{i+1} < \Delta T_{i+2}$, word 012). Simulations of the LK model including a sinusoidal modulation of the pump current parameter were found to be in good agreement with the observations, and a detailed comparison model-experiments will be reported elsewhere.

The symbolic behavior is in qualitative good agreement with the modified circle map, when the parameter K, that represents the forcing amplitude, is varied (Fig. 4b). However, the agreement is not as good as in the unperturbed situation and we interpret that this could be due to the fact that in the experiment, the current modulation introduces an additional source of noise, which probably depends on the modulation amplitude. In order to test this interpretation we considered an additional noise term in the map equation (see Methods) and, as can be seen in Fig. 4c, this term mainly affects the word probabilities at low modulation amplitudes (before the crossover), improving the agreement with the experimental probabilities (Fig. 4a). As could be expected, the symbolic behavior depends not only on the modulation amplitude, but also, on the modulation frequency, and a detailed analysis is in progress and will be reported elsewhere.

Discussion

The symbolic behavior of the modified circle map demonstrates that, with and without periodic forcing, it is an adequate minimal model for representing qualitatively the symbolic dynamics underlying the sequence of optical spikes. Considering the high-dimensionality of the laser dynamics (induced by the feedback delay time) it is unexpected and remarkable that a simple iterative model with only one variable can mimic the extended correlations present in the sequence of spikes.

Both, in the experiments and in the LK model simulations, we found the presence of two clusters of word probabilities (021-102,

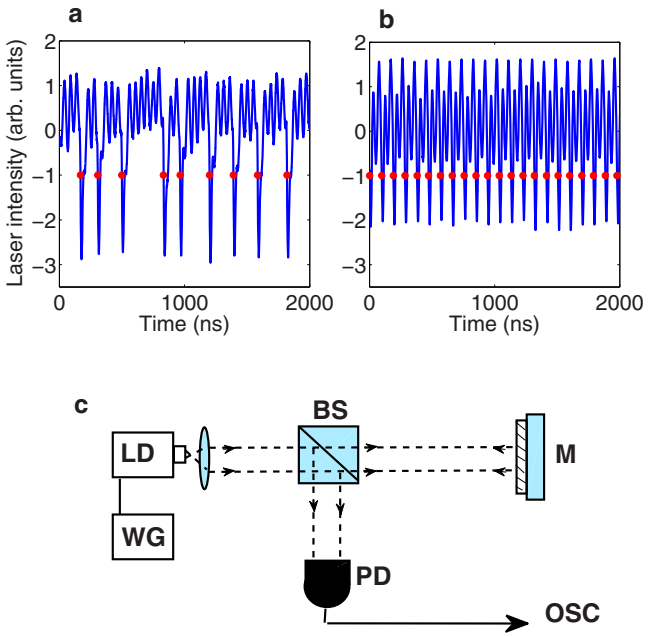

Figure 3 | Laser spiking output under external periodic forcing. Time trace of the laser intensity when the modulation amplitude is (a), 31.2 mV (1.6% of the DC current); (b), 70.2 mV (3.6% of the DC current); other parameters are as indicated in Methods. The effect of the forcing is clearly visible in the laser intensity. (c), Schematic representation of the experimental setup, where the forcing is included as a direct modulation of the laser pump current. LD stands for laser diode, WG for waveform generator, BS for beamsplitter, PD for photodetector, OSC for oscilloscope and M for mirror (see Methods).

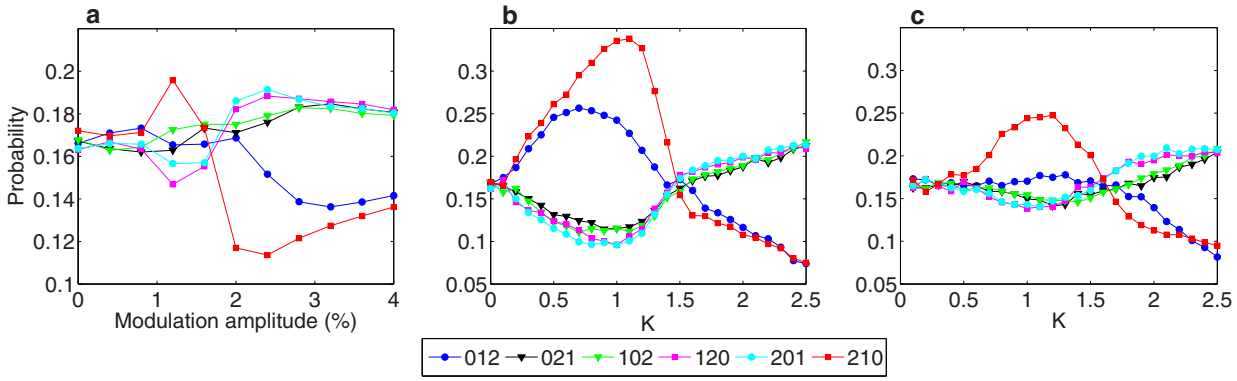

Figure 4 | Influence of periodic forcing in the organization of the symbolic patterns. (a), Probabilities computed from the experimental data. The DC value of laser pump current is 39 mA and the modulation amplitude is increased from 0 mV to 78 mV (0% to 4% of the DC current, other experimental parameters are as described in Methods). The two word clusters are clearly seen, which are the same as without modulation. A crossover in the word hierarchy can also be observed at about 1.8%. (b), Probabilities computed from the modified circle map, when varying the parameter K with constant noise strength. Here again, the hierarchical and clustered structure of the probabilities is in good qualitative agreement with that in the experimental data. The parameters are $\rho = -0.23$, $\alpha_c = 0.2$ and $\beta_c = 0.002$. (c), Probabilities computed with the modified circle map considering a noise strength that decreases with the modulation amplitude. For weak modulation the agreement with the experimental probabilities is further improved.

120-201). We also found that 012 and 210 are the most probable words, at low and high current respectively, revealing that serial correlations, among four consecutive optical spikes, vary with the laser pump current. We show in the Supplementary Information that these correlations are not detected via the standard correlation analysis. The good qualitative agreement experiment-simulations indicate that this organization of symbolic patterns is a fingerprint of the topology of the attractor underlying the LFF dynamics.

As a future study it would be interesting to consider the phenomenological model proposed by Mindlin and coworkers[23], which gives a good description of the probability distribution function of the inter-spike intervals. In the symbolic dynamics of this model the most probable words are 012 and 210[24], and it would be interesting to explore the parameter space to search for the two clusters of words uncovered here.

To summarize, we demonstrated the existence of a hierarchical organization of patterns in the symbolic dynamics of semiconductor lasers, in the spiking regime induced by delayed optical feedback. This organization displays a clustered hierarchical structure which had not been previously noticed, despite the great attention that the laser spiking output has attracted. Simulations of the LK model were found to be in good qualitative agreement with the experimental observations, providing in this way a validation of the LK model in unprecedent long time-scales. We also found a minimal model, a modified circle map, that describes the hierarchy and clustered symbolic structure. The validity of the minimal model was further demonstrated by analyzing the symbolic dynamics of the laser with periodic forcing via direct current modulation.

Since the modified circle map is a generic model of forced oscillators, we envision that the underlying symbolic structure found here could be observed in many other dynamical systems. In particular, our results could be relevant for improving our understanding of the firing patterns of biological neurons. Establishing a direct connection between these different dynamical systems can offer new perspectives, both, in photonics and in neuroscience. Since the modified circle map has been proposed as a minimal model of electroreceptors of paddlefish[18], our results suggest that optical neurons inspired in biological ones, displaying similar temporal correlations in their firing patterns, could be built using semiconductor lasers, thus providing a novel, inexpensive and controllable experimental set up for mimicking neuronal activity. In particular, the optical setup could be used to analyze the role of external forcing in the spike sequence, providing, for example, new insight in the role of gamma oscillations in the brain, which have been shown to serve to concentrate neuronal discharges to particular phases of the gamma cycle[25]. On the other hand, because semiconductor lasers are nowadays the coherent light sources used in telecommunications and data storage, and because there is a wide range of spiking regimes with experimentally controllable parameters[26], we envision that our finding could also contribute to the development of novel applications of semiconductor lasers in neuro-inspired optical computing devices[27–29].

Methods

Experimental setup. The experiments were performed with a 675 nm Al-GaInP semiconductor laser (AlGaInP Sanyo DL-2038-023) with optical feedback from a diffraction grating (see Fig. 1c). The external cavity length was 70 cm, giving a feedback delay time of 4.7 ns. A beam-splitter sends 50% of the light to a 1 GHz oscilloscope (Agilent Infiniium 9000). The laser temperature and pump current were controlled to an accuracy of 0.01 C and 0.01 mA respectively with a ITC502 Thorlabs laser diode combinator controller. The operating temperature was 18 C and the laser pump current was varied in steps of 0.1 mA, from 26.3 mA to 27.3 mA. At 18 C the threshold current of the solitary laser is $I_{th} = 27.8$ mA, and the feedback-induced threshold reduction is 6.5%. Time series of 32 ms were recorded (3.2×10^7 data points), containing 70,000–300,000 spike events, for low and high pump current respectively.

To study the dynamics under periodic forcing, a Hitachi HL6714G diode laser was used, lasing at 650 nm, with solitary threshold of $I_{th} = 38$ mA. The pump current was set to 39 mA, and optical feedback resulted in a threshold reduction of 8%. The external cavity length was of 70 cm, giving a time delay of 4.7 ns. The pump current was modulated through a bias-tee in the laser mounting and with an 80 MHz waveform generator (Agilent 33250A). The modulation frequency was 17 MHz and the modulation amplitude was varied in the range 0% to 4% (78 mV), relative to the DC value of 39 mA ($1.03I_{th}$). Time series of 20 ms were recorded, which contained between 70,000 and 200,000 spike events, for low and high modulation amplitude respectively.

Ordinal time-series analysis. The time series of inter-spike intervals, $\{\Delta T_i\}$, were analyzed using the ordinal method[11], which takes into account the order in which the values appear in the time series. As this method is well known, we only describe it briefly.

A time series $\{x(t)\}$ of length N is divided in $N - D$ vectors of length D, and each element of a vector is replaced by a number from 0 to $D - 1$, in accordance with the relative length of the element in the ordered vector (0 corresponding to the shortest and $D - 1$ to the longest value in each vector). In this way, each vector has associated an "ordinal pattern" (or word) composed of D symbols. For example, with $D = 3$, the vector $\{x(t), x(t + 1), x(t + 2)\} = \{5, 1, 10\}$ gives the word 102, because $x(t + 1) < x(t) < x(t + 2)$. Then, by counting the frequency of occurrence of the different words, their probabilities are computed. To perform an statistically significant analysis, the number of data points in the time series should be $N \gg D!$. This condition is fulfilled as we perform the analysis with $D = 2$, 3, and 4, and in our datasets N is between 70,000 and 300,000.

In all the figures the probabilities of the words have been computed considering a rolling-window. Specifically, for $D = 3$ ($D = 2$) the time-series of inter-spike intervals, $\{\Delta T_1, \Delta T_2 \ldots, \Delta T_N\}$, was transformed into 3 (2) symbolic sequences by considering 3 (2) different initial ΔT values for encoding the words. For example, for $D = 3$, in one sequence the words are formed as $(\Delta T_1, \Delta T_2, \Delta T_3)$, $(\Delta T_4, \Delta T_5, \Delta T_6)$, etc. In the second

sequence as (ΔT_2,ΔT_3,ΔT_4), (ΔT_5,ΔT_6,ΔT_7), etc. And in the third sequence as (ΔT_3,ΔT_4,ΔT_5), (ΔT_6,ΔT_7,ΔT_8), etc. From each of these sequences, the probabilities of the words were computed, an then, they were averaged before plotting the results. This is fully equivalent to consider overlapping patterns (i.e., a single symbolic sequence formed as (ΔT_1, ΔT_2, ΔT_3), (ΔT_2, ΔT_3, ΔT_4), etc.)

Compared with other symbolic methods, the ordinal transformation has the advantage that the symbolic sequence keeps the information about the correlations present in the time-series, but it has the drawback that the information about the actual values (i.e., the precise duration of the inter-spike intervals) is lost. However, this drawback is in fact an advantage in our case, as it allows using a simple thresholding method to determine the spike times. Because the spikes have fluctuating amplitude (particularly at low pump currents, see Fig. 1a), a simple threshold might give rise to timing errors; however, with ordinal analysis the precise values of the intervals are disregarded (as only the relative order of consecutive intervals is considered); therefore, with the ordinal transformation there is no need of using methods more sophisticated than thresholding to precisely determine the timing of the events. While the threshold chosen determines the number of spikes detected, and thus, the symbolic sequence of ordinal patterns obtained, in the Supplementary Information we also demonstrate that our findings are robust, with the hierarchical and clustered structure of word probabilities persisting in a wide-range of threshold values.

The LK model. The Lang and Kobayashi (LK) model[15] consists of two coupled delay-differential rate equations governing the evolution of the slowly varying complex electric field amplitude, E, and the carrier density, N. The model equations are:

$$\frac{dE}{dt} = \frac{1}{2\tau_p}(1+\alpha)(G-1)E + \eta E(t-\tau)e^{-i\omega_0\tau} + \sqrt{2\beta_{sp}}\xi, \quad (1)$$

$$\frac{dN}{dt} = \frac{1}{\tau_N}\left(\mu - N - G|E|^2\right), \quad (2)$$

where τ_p and τ_N are the photon and carrier lifetimes respectively, α is the linewidth enhancement factor, G is the optical gain, $G = N/\left(1+\epsilon|E|^2\right)$ (with ϵ being a saturation coefficient), μ is the pump current parameter, η is the feedback strength, τ is the feedback delay time, $\omega_0\tau$ is the feedback phase, β_{sp} is the noise strength, representing spontaneous emission, and ξ is a Gaussian distribution with zero mean and unit variance.

Typical values of the parameters were used in the simulations: $k = 300\ \mathrm{ns}^{-1}$, $\gamma = 1\ \mathrm{ns}^{-1}$, $\epsilon = 0.01$, $\tau = 5$ ns, and $\beta_{sp} = 10^{-4}\ \mathrm{ns}^{-1}$; in Figs. 2a and 2b the pump current, μ, is the control parameter and the simulations were performed with two sets of parameters which were found to give good agreement with the experimental data (in Fig. 2a, $\eta = 10\ \mathrm{ns}^{-1}$, $\alpha = 4$; in 2b, $\eta = 20\ \mathrm{ns}^{-1}$, $\alpha = 4.5$). Because the LK model is a simple model (it takes into account only one reflection in the external cavity, it neglects multi-mode emission, spatial effects, and thermal effects; in particular the shift of the emission wavelength with increasing current due to Joule heating), only a qualitative agreement could be expected.

Within the framework of the LK model it has been shown that the optical spikes are often a transient dynamics, even when noise is included in the simulations, and the duration of the transient increases with the pump current parameter[17]. In order to compute long time series of inter-dropout intervals, when the trajectory found a stable fixed point the simulation was re-started with new random initial conditions. Simulations of 2 milliseconds were performed, obtaining time series containing between 12,000 and 48,000 events, for low and high pump currents, respectively.

Minimal model. The modified circle map proposed by Neiman and Russell[19] to describe serial correlations in electroreceptors of paddlefish was found to display the same symbolic organization as that found of the spiking output of the laser with feedback, with and without periodic forcing. The map equation is:

$$\phi(i+1) = \phi(i) + \rho + \frac{K}{2\pi}[\sin(2\pi\phi(i)) + \alpha_c\ \sin(4\pi\phi(i))] + \beta_c\xi(i) \quad (3)$$

The parameter ρ is proportional to the ratio between the period of the forcing and the natural period of the oscillator, K is proportional to the forcing amplitude, α_c represents the strength of a second harmonic component, and β_c represents the strength of stochastic fluctuations (ξ being a Gaussian white noise). Considering that the values $\phi(i)$ can represent the spike times, we analyzed the time series of phase increments, $\phi(i+1) - \phi(i)$, in analogy with the inter-spike intervals, ΔT_i. As Figs. 2c and 4c show, varying the parameters α_c and K correspond to varying the laser pump current and the modulation amplitude, respectively. To take into account the additional noise introduced by the external forcing, a noise term inversely proportional to the modulation amplitude $[\beta_c(1 + 1/K)\xi(i)]$ is considered in Fig. 4d.

1. Ikegaya, Y. *et al.* Synfire chains and cortical songs: temporal modules of cortical activity. *Science* **304**, 559–564 (2004).
2. Pedaci, F., Huang, Z., Van Oene, M., Barland, S. & Dekker, N. H. Excitable particles in an optical torque wrench. *Nature Phys.* **7**, 259 (2011).
3. Amador, A., Sanz Perl, Y., Mindlin, G. B. & Margoliash, D. Elemental gesture dynamics are encoded by song premotor cortical neurons. *Nature* **495**, 59–64 (2013).
4. Orlandi, J. G., Soriano, J., Alvarez-Lacalle, E., Teller, S. & Casademunt, J. Noise focusing and the emergence of coherent activity in neuronal cultures. *Nature Phys.* **9**, 582–590 (2013).
5. Parlitz, U. *et al.* Classifying cardiac biosignals using ordinal patterns statistics and symbolic dynamics. *Comp. Biol. Med.* **42**, 319 (2012).
6. Schindler, K. *et al.* Forbidden ordinal patterns of periictal intracranial EEG indicate deterministic dynamics in human epileptic seizures. *Epilepsia* **52**, 1771 (2011).
7. Davidsen, J. & Kwiatek, G. Earthquake interevent time distribution for induced micro-, nano-, and picoseismicity. *Phys. Rev. Lett.* **110**, 068501 (2013).
8. Wu, Y., Zhou, C., Xiao, J., Kurths, J. & Schellnhuber, J. H. Evidence for a bimodal distribution in human communication. *PNAS* **107**, 18803 (2010).
9. Rybski, D., Buldyrev, S. V., Havlin, S., Liljeros, F. & Makse, H. A. Communication activity in a social network: relation between long-term correlations and inter-event clustering. *Sci. Rep.* **2**, 560 (2012).
10. Hicke, K., Porte, X. & Fischer, I. Characterizing the deterministic nature of individual power dropouts in semiconductor lasers subject to delayed feedback. *Phys. Rev. E* **88**, 052904 (2013).
11. Bandt, C. & Pompe, B. Permutation entropy: a natural complexity measure for time series. *Phys. Rev. Lett.* **88**, 174102 (2002).
12. Zanin, M., Zunino, M., Rosso, O. A. & Papo, D. Permutation entropy and its main biomedical and econophysics applications: a review. *Entropy* **14**, 1553 (2012).
13. Amigo, J. M., Keller, K. & Kurths, J. Recent progress in symbolic dynamics and permutation complexity: ten years of permutation entropy. *Eur. Phys. J. Spec. Top.* **222**, 2 (2013).
14. Toomey, J. P. & Kane, D. M. Mapping the dynamic complexity of a semiconductor laser with optical feedback using permutation entropy. *Opt. Exp.* **22**, 1713 (2014).
15. Soriano, M. C., García-Ojalvo, J., Mirasso, C. R. & Fischer, I. Complex photonics: dynamics and applications of delay-coupled semiconductor lasers. *Rev. Mod. Phys.* **85**, 421 (2013).
16. Lang, R. & Kobayashi, K. External optical effects on semiconductor injection laser properties. *IEEE J. Quantum Electron.* **16**, 347 (1980).
17. Torcini, A., Barland, S., Giacomelli, G. & Marin, F. Low-frequency fluctuations in vertical cavity lasers: experiments versus Lang-Kobayashi dynamics. *Phys. Rev. A* **74**, 063801 (2006).
18. Zamora-Munt, J., Masoller, C. & García-Ojalvo, J. Transient low-frequency fluctuations in semiconductor lasers with optical feedback. *Phys. Rev. A* **81**, 033820 (2010).
19. Neiman, A. B. & Russell, D. F. Models of stochastic biperiodic oscillations and extended serial correlations in electroreceptors of paddlefish. *Phys. Rev. E.* **71**, 061915 (2005).
20. Aragoneses, A., Rubido, N., Tiana-Alsina, J., Torrent, M. C. & Masoller, C. Distinguishing signatures of determinism and stochasticity in spiking complex systems. *Sci. Rep.* **3**, 1778 (2013).
21. Sukow, D. W. & Gauthier, D. J. Entraining power-dropout events in an external-cavity semiconductor laser using weak modulation of the injection current. *IEEE J. Quantum Electron.* **36**, 175 (2000).
22. Lam, W.-S., Guzdar, P. N. & Roy, R. Effect of spontaneous emission noise and modulation on semiconductor lasers near threshold with optical feedback. *Int. J. of Modern Phys. B* **17**, 4123 (2003).
23. Yacomotti, A. M. *et al.* Interspike time distribution in noise driven excitable systems. *Phys. Rev. Lett.* **83**, 292 (1999).
24. Rubido, N., Tiana-Alsina, J., Torrent, M. C., Masoller, C. & García-Ojalvo, J. Language organization and temporal correlations in the spiking activity of an excitable laser: Experiments and model comparison. *Phys. Rev. E* **84**, 026202 (2011).
25. Nikolic, D., Fries, P. & Singer, W. Gamma oscillations: precise temporal coordination without a metronome. *Trends in Cognitive Sciences* **17**, 54 (2013).
26. Junges, L., Pöschel, T. & Gallas, J. A. C. Characterization of the stability of semiconductor lasers with delayed feedback according to the Lang-Kobayashi model. *Eur. Phys. J. D* **67**, 149 (2013).
27. Hurtado, A., Schires, K., Henning, I. D. & Adams, M. J. Investigation of vertical cavity surface emitting laser dynamics for neuromorphic photonic systems. *Appl. Phys. Lett.* **100**, 103703 (2012).
28. Fok, M. P., Tian, Y., Rosenbluth, D. & Prucnal, P. R. Pulse lead/lag timing detection for adaptive feedback and control based on optical spike-timing-dependent plasticity. *Opt. Lett.* **38**, 419 (2013).
29. Nahmias, M. A., Shastri, B. J., Tait, A. N. & Prucnal, P. R. A leaky integrate-and-fire laser neuron for ultrafast cognitive computing. *IEEE J. Sel. Top. in Quantum Electron.* **19**, 1800212 (2013).

Acknowledgments

The authors are grateful to Professor Daniel J. Gauthier for his guidance regarding the experimental setup. C.M. acknowledges inspiring discussions with U. Parlitz and O.A. Rosso regarding ordinal analysis. This work was supported in part by grant FA8655-12-1-2140 from EOARD US, grant FIS2012-37655-C02-01 from the Spanish MCI, and grant 2009 SGR 1168 from the Generalitat de Catalunya. C.M. acknowledges partial support from the ICREA Academia programme.

Author contributions

A.A. and T.S. performed the experiments, S.P. performed the numerical simulations, A.A. and C.M. analyzed the data and wrote the manuscript text, M.C.T. and C.M. supervised the research. All authors reviewed the manuscript.

Additional information

Supplementary information accompanies this paper at http://www.nature.com/scientificreports

Competing financial interests: The authors declare no competing financial interests.

How to cite this article: Aragoneses, A., Perrone, S., Sorrentino, T., Torrent, M.C. & Masoller, C. Unveiling the complex organization of recurrent patterns in spiking dynamical systems. *Sci. Rep.* **4**, 4696; DOI:10.1038/srep04696 (2014).